Event-based, Water-induced Soil Erosion Modeling for Medium Watersheds in Yen Bai province, Vietnam Using the KINEROS2 Model

Hong Quang NGUYEN, Vietnam; Martin KAPPAS, Germany

Key words: Water-induced soil erosion; KINEROS2; Sediment yield, flow; Discharge; Yen Bai

SUMMARY

The problem of water, soil erosion has become an important issue in the North of Vietnam. Modeling its processes might help better understanding and quantifying the development of erosion. Based on data availability, climate condition and scale (medium watershed and event-based rain) we decided to use the KINEROS2 model for this research. The changing in land use practices has significant impact on reduction of saturated hydraulic conductivity (Ks), thus, increases the Horton overland flow (HOF) and eventually exaggerates soil erosion. On the model simulation stage, we found that the boundary conditions and the parameter sensitive tests were crucial for estimation of model outputs, these converged to measured data. Interestingly, the use of finer temporal resolution (5 minutes) of radar rainfall (accumulative 144 mm) produced much lower sediment yield (SeY) rates comparing to satellite precipitation (30 minutes, accumulative 138 mm). Although each tested variable had different effects on model outputs, the Ks presented a most sensitive parameter to SeY in both channels and on planes, following by soil saturation index (S) and hillslope roughness (R). The geomorphological resolutions based on critical source area (CSA) defining modeling resolutions were founded remarkable for estimation soil loss and must be determined with care. Finally, changing in land uses resulted in soil erosion was mapped with significant rises in SeY for whole Man Kim and in some areas in Nam Khat watershed.

Event-based, Water-induced Soil Erosion Modeling for Medium Watersheds in Yen Bai province, Vietnam Using the KINEROS2 Model

Hong Quang NGUYEN, Vietnam; Martin KAPPAS, Germany

1. INTRODUCTION

Land degradation, including soil erosion has become one of the most serious problems (da Silva et al., 2012; Kefi et al., 2011; Pham Thai NAM, 2003) and effected sustainable development (Kefi et al., 2012), particularly in developing countries with low cultivated land per capita as in Vietnam. Information about the rate of soil erosion could help better understanding the development of the land (Parsons et al., 2004) and is useful for determining the sustainability of agricultural practices (Cooper et al., 2012). Effective soil erosion modeling can provide important data on soil erosion patterns and trends (Millington, 1986). In northern Vietnam, the problem of land degradation has reportedly become worst due to reduction of canopy mostly the decline of forested land (shifting agriculture and timber removal by ethnic groups) (Tuan, 1993) and forest fragmentation (Ziegler et al., 2006). This has reduced the saturated hydraulic conductivity (Ks) of the lands (forest land has highest Ks among the others), and thus, increased the Hortonian overland flow (HOF, occurred when the rainfall rate exceeds infiltration capacity and surface storage; (Horton, 1933)). Two watersheds named Nam Kim and Nam Khat; both located in the Mu Cang Chai district of Yen Bai province, Vietnam were chosen for the case study based on the high rates of soil erosion (about 5-10 ton h^{-1} y^{-1}) derived from study results of Quang and Kappas (2015) using SWAT model.
There are various existing methods approaching to the erosion issue (Guzman et al., 2013), including direct and indirect approaches. Modeling is one of the options which might have some advantages in terms of time consuming, cost and trend analyses. The KINEROS2 model accounts separately for soil erosion caused by rain drop energy and by flowing water (Woolhiser et al., 1990). On the other hand, (SWAT (Arnold, 1994) model accounts only runoff causing erosion, WEPP model divides erosion process into rill and interill erosion (Nearing et al., 1989)). In KINEROS2, some key parameters are taken into account as Ks, Manning n, splash, cover, soil profiles (fraction of sand, silk and clay) etc. Although each variable has different extend of sensitivity to model’s outputs, all these parameters must be well-prepared in order to gain best model estimations. Additionally, observed data is crucial and prerequisite for validating the model. We applied the KINEROS2 for modeling sediment yield on hill slopes and sediment transport in channels of two medium size watersheds with model validation, sensitivity tests and trend analysis of different LULCs. While this KINEROS2 was developed for small semi-arid watersheds (Burns et al., 2008), it was employed for tropics which are similar to our study site as a study of Ziegler et al., (2007). Furthermore, based on our study aim of spatial and temporal scale of modeling, we decided to use the model.
In this study, we investigate the ability of KINEROS2 to model medium size (74-268 km^2) catchment areas with acceptable results. Herein, we (1) calibrate channel discharge at the outlets and compare with gauged data with different uses of rainfall data sources; (2)

parameter sensitive test for some variables; (3) analysis the effect of LULC inputs on sediment yield in watershed's elements and streams. The results indicated that the model was validated by producing the discharge closely to field measured data for both uses of satellite and radar rainfalls. What is more, we found that the tests for parameter sensitivities were crucial for understanding the model behaviors and in what aspects each variable had an influence on hydraulic responses in the watersheds. Therefore, we recommend the use of KINEROS2 for the similar study objectives.

2. STUDY SITE

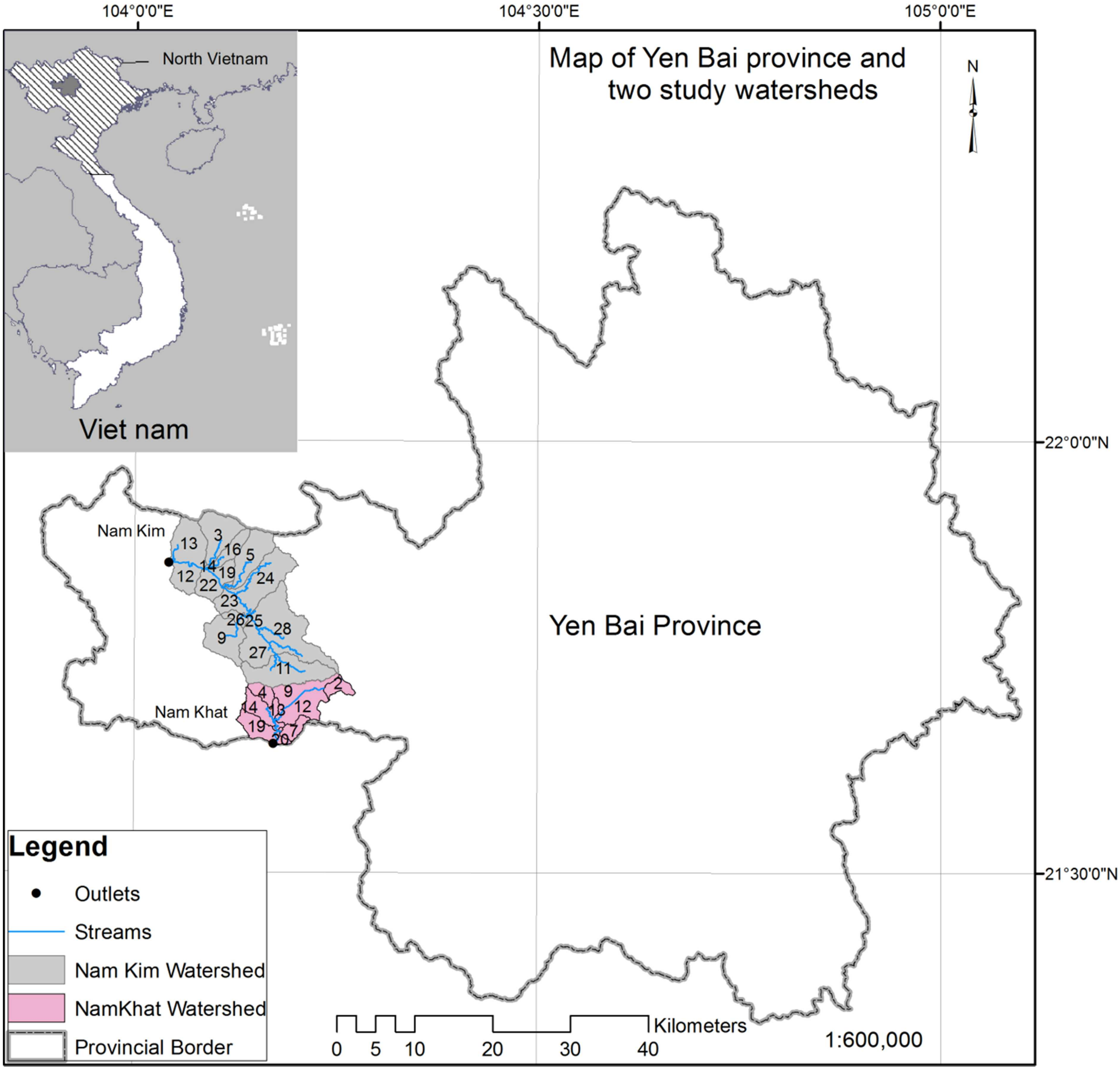

Figure 1: Site study - Nam Kim and Nam Khat watershed of Yen Bai province, Vietnam.

The study watersheds are located in Yen Bai province, Vietnam (Fig. 1) and are a part of typical tropics in North-Western Vietnam. The areas of the watershed are 268 km2 and 74 km2 for Nam Kim and Nam Khat watershed, respectively. The central coordinates of the province are 104°30'9.0" E and 21°35'26.7" N and the mean elevation is about 900 meters above the Bien Dong Sea level. The annual precipitation in the region varies from 1365 to 1570 mm. About 85 percent of the total rainfall is recorded in the summer time. The mean daily solar radiation is estimated very high at 14.5 (MJ m^{-2} d^{-1}) and the mean wind speed is 1.23 (m s^{-1}). We chose these watersheds for the case study because of a representation of rapid eroded processes in there and their representative morphological characteristics of the whole region.

3. MATRERIALS AND METHOD

3.1. Soil Erosion Equations used in KINEROS2 model

KINEROS2 (Smith et al., 1995) is a modified model of the original model of KINEROS (Woolhiser et al., 1990) and is an event-based model rather than a continuous simulation model (Smith et al., 1999). It is a model of Hortonian hydrology and simulates saturation overland flow when the top soil layer lying above a restrictive layer becomes saturated. While the SWAT model calculates sediment yield based on the amount of runoff and employs the equation of (Williams, 1995), KINROS2 estimates sediment transport based on both rain-drop energy and surface runoff. Soil erosion and sediment transport rate are determined by the solution to the sediment balance as the following relation (Smith et al., 1999);

$$\frac{\partial(AC_S)}{\partial t} + \frac{\partial(QC_S)}{\partial x} - we(x,t,C_s) = q_c(x,t) \qquad \textbf{(1)}$$

Where, $\boldsymbol{A}$ is local cross sectional area of flow (m^2), $\boldsymbol{Q}$ is local discharge rate m^3 s^{-1}, $\boldsymbol{t}$ is time (s), $\boldsymbol{x}$ is distance along the flow path (m), $\boldsymbol{w}$ indicates local flow width (m), $\boldsymbol{q}$ is rainfall exceed (m s^{-1}), $\boldsymbol{C_s}$ is the sediment concentration (m^3/m^3), $\boldsymbol{e}$ indecates the local rate of erosion or deposition (m^3 s^{-1} m^{-2}) and $\boldsymbol{q_c}$ refers to the rate of sediment inflow, as for lateral inflow to a channel (m s^{-1}).

In which, KINEOS2 estimates runoff by dynamic routing of rainfall excess;

$$q_{(t)} = r_{(t)} - f_{(t)} \qquad \textbf{(2)}$$

Where, $\boldsymbol{r_{(t)}}$ is rainfall runoff pattern (mm s^{-1}), $\boldsymbol{f_{(t)}}$ indicates infiltration pattern usually more effectively related to infiltrate depth (mm s^{-1}).

In addition, erosion rate is computed from rain splash erosion $\boldsymbol{e_s(r,h)}$ and hydraulic erosion, $\boldsymbol{e_h}$**,** rain flash erosion is directly linked to rain energy and related to rain intensity in a unit of area. KNEROS2 links $\boldsymbol{e_s}$ with precipitation rate (r), the fraction of covered soil (y) and the min runoff depth $(\bar{h})$.

Splash erosion is determined as follows;

$$e_s = Spl\,(1-y)exp(-c_d\bar{h})r^2 \qquad \textbf{(3)}$$

The soil vulnerability to rainfall detachment is determined by parameter $\boldsymbol{Spl}$, $\boldsymbol{c_d}$ indicates the effect of water depth in damping splash energy. A reduction in splash erosion with a raising depth of surface water is expressed by the exponent function and reflecting its dampening effect on splash energy.

The hydraulic erosion is calculated as in relation;

$$e_h = Ch_{vs}\,(C_m - C_s) \qquad \textbf{(4)}$$

Where, $\boldsymbol{C_m}$ is transport capacity, presents a concentration and is estimated in KINEROS2 by a modified form of the Engelund and Hansen relation (Engelund & Hansen, 1967). The $\boldsymbol{Ch}$ is a coefficient and inversely related to soil cohesion or any other restriction on soil entrainment by flowing water. It is set to 1.0 during the deposition process ($\boldsymbol{C_s}$>$\boldsymbol{C_m}$). Schematic illustration of the geometric subdivision of a hypothesis catchment and other components of the model can be referenced in the literature of (Woolhiser et al., 1990).

3.2. Data for the model parameterizations

3.2.1 The Digital Elevation Model (DEM)

A DEM extracted from a Yen Bai database (produced by the Vietnam Natural Resources and Environment Corporation in 2009) was used for morphological input data. This is a 10x10 m grid-based DEM and produced using Photogrammetry technology (Image Stations of Intergraph Corporation, USA).

3.2.2 Land use and land cover (LULC) datasets

We used Landsat TM imagery for LULC classifications and the ground control points and ground-truth data were extracted from the Yen Bai geodatabase for geometric corrections and the supervised maximum likelihood classified method using the ENVI 4.7, respectively. Two Landsat TM scenes acquired on 28th January 2002 and 26th March 2007 were processed and analyzed for seven LULC categories (Fig. 9) and accuracy assessment (kappa statistics producer accuracy and user accuracy).
Mean producer accuracy of classes of LULC2002 is 69.01%, of LULC2007 is 72.70 %. Average user accuracy calculated for LULC2002 and 2007 are 68.99 and 72.81% and overall accuracies are 69.3 and 72.2 %, respectively. The kappa statistics were also estimated at 0.65 for LULC2002 and 0.69 for LULC2007. The reductions of vegetation cover presenting in the watersheds during 2002-2007 period might be seen within the Fig. 9. This, on the one hand, is illustrated most clearly in the Nam Kim and less, in the other hand, in Nam Khat watershed.

3.2.3 Soil data

Soil profiles of the study site were derived from Yen Bai custom soil map scale 1: 600,000 (Fig. 2) produced by the Environment and Resource Centre-Agricultural Institute of Plan and Design, Vietnam. The soils were mapped in MapInfo software in 1996 and categorized into 6 major soil groupings including fluvisols, calcisols, ferralsols, alisols, acrisols and gleysols.

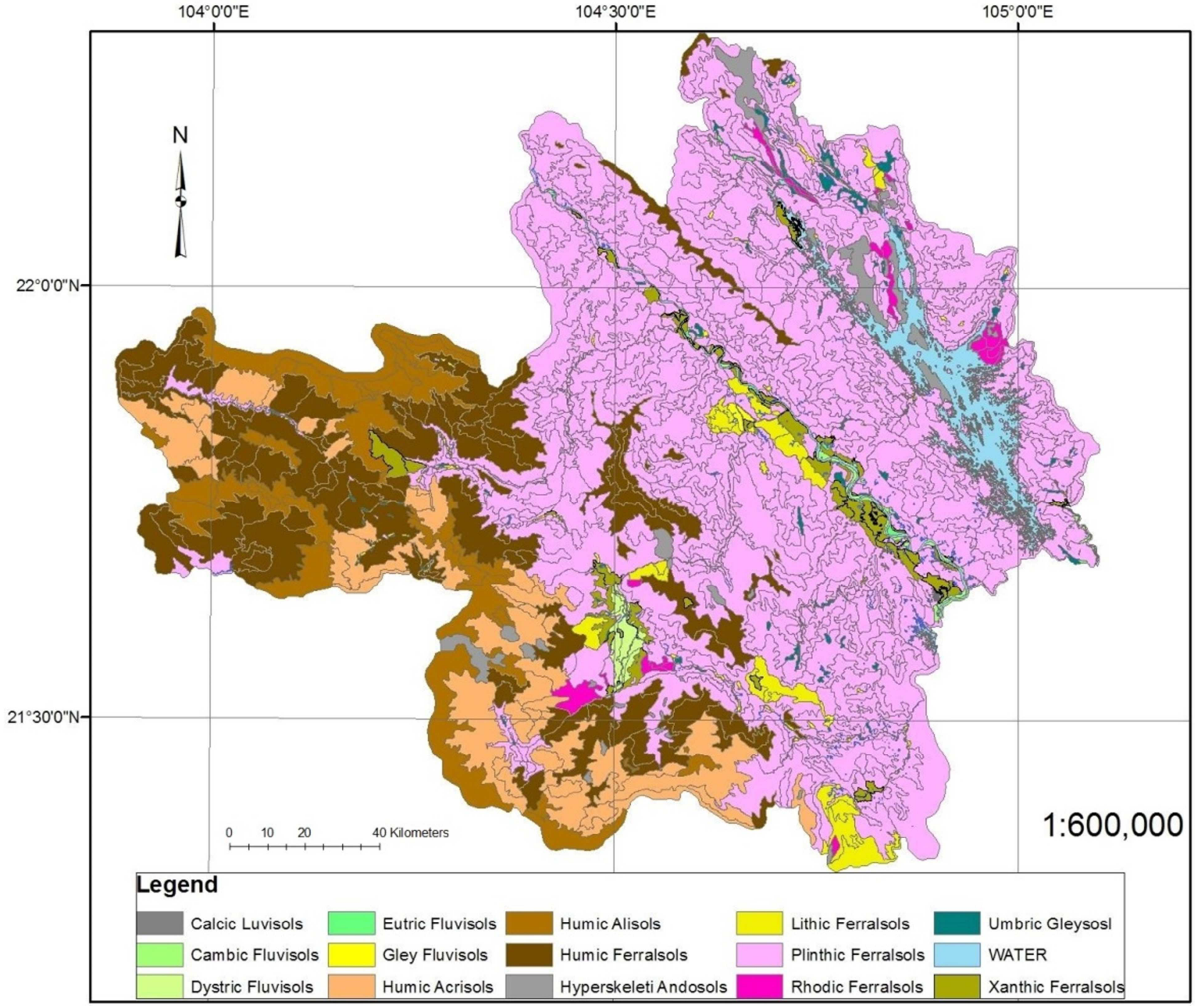

Figure 2: Soil classification map of Yen Bai province.

3.2.4 Satellite-based and radar rainfall data

MTSAT images with fifteen-minute and 2x2 km temporal and spatial resolutions were provided by the Japanese Meteorological Satellite Center (NCHMF) for the rainfall input to the model in order to assess the rain event on 23rd June 2011. The radar rainfall with five-minute, 1x1 km rainfall images from the NCHMF were used for the precipitation input for the same day.

3.2.5 Observed discharge for model validation

Only discharge data from the hydrological gauge on the outlet of Nam Kim watershed called Mu Cang Chai station was available at collected for the model validation. There was another gauge on Hut's outlet, but Hut basin is too big (≈ 617 km^2) and considered not appropriate for KINEROS2 application due to scale problem.

3.3. Application of the model

3.3.1 Watershed delineations and parameterizations

The two watersheds were parameterized using above inputs and the tabular summaries are indicated within table 1 and 2. The information within the two tables is using LULC2007 and the CSAs were set 7.5 % of the area for Nam Kim and 5% for Nam Khat watershed.

3.3.2 Testing model sensitive parameters

As based on previous literatures, the K_S- saturated hydraulic conductivities of hill slopes presented to be most sensitive to surface runoff (Hadi Memarian et al., 2012). The sensitivities of the relative saturation index (R) and the critical source area (CSA) are considered to have significant effects on the model outputs (Kalin et al., 2003). Therefore, we tested these parameters for our study zones.

3.3.3 Model calibration and validation

The watersheds were calibrated with a slope adjustment for the curve number (CN) of the nine land use types of both LULC2002 and 2007 for the aim of estimates the soil erosion of the single rain event on 23rd June 2011. The sensitive parameters (section 2.4b) were altered for every model run for the single rain. The relative soil saturation index (S) must be pre-defined as antecedent condition and obtained from the literature (Quang et al., 2015, reviewing on the Hydrological Sciences Journal). The S values were set at 0.46 for Nam Kim and 0.42 for Nam Khat. The method of accuracy assessment was to estimate the goodness of model simulation based on the Nash and Sutcliffe efficiency (Nash & Sutcliffe, 1970).

Table 1: Parameters of the Nam Kim watershed

Plane_ID	Shape_Area	AvgSlope	INT_	Cover	Mann_N	Splash	Rock	Ks	G	Por	Smax	Cv	Fract_sand	Fract_silt	Fract_clay	Dist
3	21.6	0.59	1.68	44.66	0.08	121.91	0.07	5.41	300.91	0.44	0.84	0.52	0.36	0.25	0.39	0.27
5	21.6	0.62	1.47	39.15	0.06	121.89	0.07	5.14	298.69	0.44	0.84	0.53	0.37	0.25	0.38	0.28
9	22.4	0.53	2.01	50.10	0.09	120.13	0.06	4.36	334.32	0.46	0.83	0.50	0.28	0.23	0.48	0.22
11	32.6	0.52	1.71	56.25	0.10	119.26	0.06	4.08	346.43	0.46	0.83	0.50	0.26	0.22	0.51	0.21
12	12.3	0.58	1.65	56.90	0.10	120.15	0.06	5.24	334.99	0.46	0.84	0.51	0.27	0.23	0.50	0.21
13	22.8	0.59	2.03	42.79	0.07	122.46	0.06	6.72	266.34	0.42	0.84	0.58	0.48	0.25	0.27	0.35
14	0.2	0.63	1.80	35.92	0.05	122.94	0.06	8.08	291.95	0.47	0.86	0.56	0.30	0.24	0.46	0.21
16	8.9	0.66	1.48	50.50	0.08	120.71	0.07	4.86	323.63	0.45	0.84	0.51	0.31	0.24	0.46	0.23
17	0.3	0.50	1.65	42.35	0.05	119.93	0.06	4.69	337.11	0.47	0.84	0.52	0.26	0.23	0.51	0.20
18	0.6	0.63	1.21	43.46	0.04	122.64	0.05	7.58	254.08	0.41	0.84	0.61	0.51	0.25	0.23	0.37
19	6.6	0.54	1.51	43.33	0.05	121.03	0.06	6.00	301.30	0.44	0.84	0.56	0.37	0.24	0.39	0.28
22	9.7	0.57	1.63	52.00	0.08	119.98	0.06	4.97	338.77	0.47	0.84	0.52	0.26	0.23	0.51	0.20
23	8.5	0.57	1.75	48.24	0.08	119.07	0.06	3.50	354.30	0.47	0.83	0.49	0.24	0.22	0.54	0.19
24	30.4	0.59	1.64	55.32	0.10	122.32	0.06	6.60	284.45	0.43	0.84	0.54	0.41	0.25	0.33	0.31
25	1.3	0.57	1.72	53.20	0.09	118.39	0.06	3.11	367.13	0.47	0.83	0.49	0.21	0.22	0.57	0.17
26	2.7	0.54	2.21	35.20	0.05	118.81	0.06	2.86	359.16	0.47	0.83	0.49	0.23	0.22	0.55	0.18
27	17.3	0.52	1.80	51.75	0.09	118.57	0.06	3.21	363.51	0.47	0.83	0.49	0.22	0.22	0.56	0.18
28	48.5	0.56	1.72	51.61	0.09	120.18	0.06	4.57	330.62	0.46	0.83	0.51	0.30	0.23	0.47	0.23

Table 2: Parameters of the Nam Khat watershed

Plane_ID	Shape_Area	AvgSlope	INT_	Cover	Mann_N	Splash	Rock	Ks	G	Por	Smax	Cv	Fract_sand	Fract_silt	Fract_clay	Dist
2	5.92	0.51	1.65	72.56	0.12	122.07	0.06	7.93	295.79	0.44	0.84	0.55	0.38	0.25	0.37	0.28
4	5.94	0.56	2.18	65.88	0.10	122.27	0.05	7.99	258.82	0.40	0.83	0.59	0.53	0.25	0.22	0.39
7	6.08	0.47	2.28	63.27	0.09	121.38	0.05	7.17	268.12	0.40	0.83	0.59	0.52	0.25	0.23	0.39
9	13.63	0.41	2.21	58.91	0.08	121.18	0.06	6.81	293.34	0.43	0.83	0.59	0.42	0.24	0.34	0.32
12	16.05	0.42	1.67	67.07	0.11	119.45	0.06	5.09	337.19	0.45	0.83	0.53	0.30	0.23	0.48	0.23
13	2.37	0.45	2.64	55.41	0.06	121.54	0.05	6.78	263.00	0.40	0.83	0.60	0.54	0.25	0.21	0.40
14	9.02	0.60	1.88	69.63	0.11	123.16	0.06	8.93	250.57	0.40	0.84	0.58	0.53	0.26	0.21	0.39
15	0.29	0.53	2.73	52.07	0.05	121.54	0.05	6.54	263.00	0.40	0.83	0.60	0.54	0.25	0.21	0.40
16	0.88	0.54	2.67	58.52	0.07	121.54	0.05	7.00	263.00	0.40	0.83	0.60	0.54	0.25	0.21	0.40
17	0.03	0.51	3.00	55.00	0.06	121.54	0.05	6.75	263.00	0.40	0.83	0.60	0.54	0.25	0.21	0.40
18	0.23	0.51	1.97	42.16	0.05	121.54	0.05	5.90	263.00	0.40	0.83	0.60	0.54	0.25	0.21	0.40
19	11.45	0.56	1.92	68.60	0.11	123.34	0.06	8.94	249.20	0.40	0.84	0.58	0.53	0.26	0.21	0.39
20	2.02	0.54	2.21	63.97	0.09	121.54	0.05	7.41	263.00	0.40	0.83	0.60	0.54	0.25	0.21	0.40

Plane_ID presents the identifications of planes (Fig. 1), Shape_Area is plane's area (km^2), AvgSlope is the zonal mean slope of the plane element in percent rise, INT_ is interception depth (m), Cover is fraction of surface covered by intercepting cover – the rainfall intensity is reduced by this fraction until the specified interception depth has been accumulated (0-1), Mann-N is Manning n coefficient, Splash represents rain splash coefficient (0-1), Rock is volumetric rock fraction, G is the mean capillary drive (mm), Por indicates soil porosity (cm^3 cm^{-3}), Smax is maximum relative saturation (%), Cv is coefficient of variation, Fract_sand, silt and clay indicates the fractions of sand silt and clay (0-1) and Dist is pore size distribution index.

4. RESULTS

4.1. Model validation

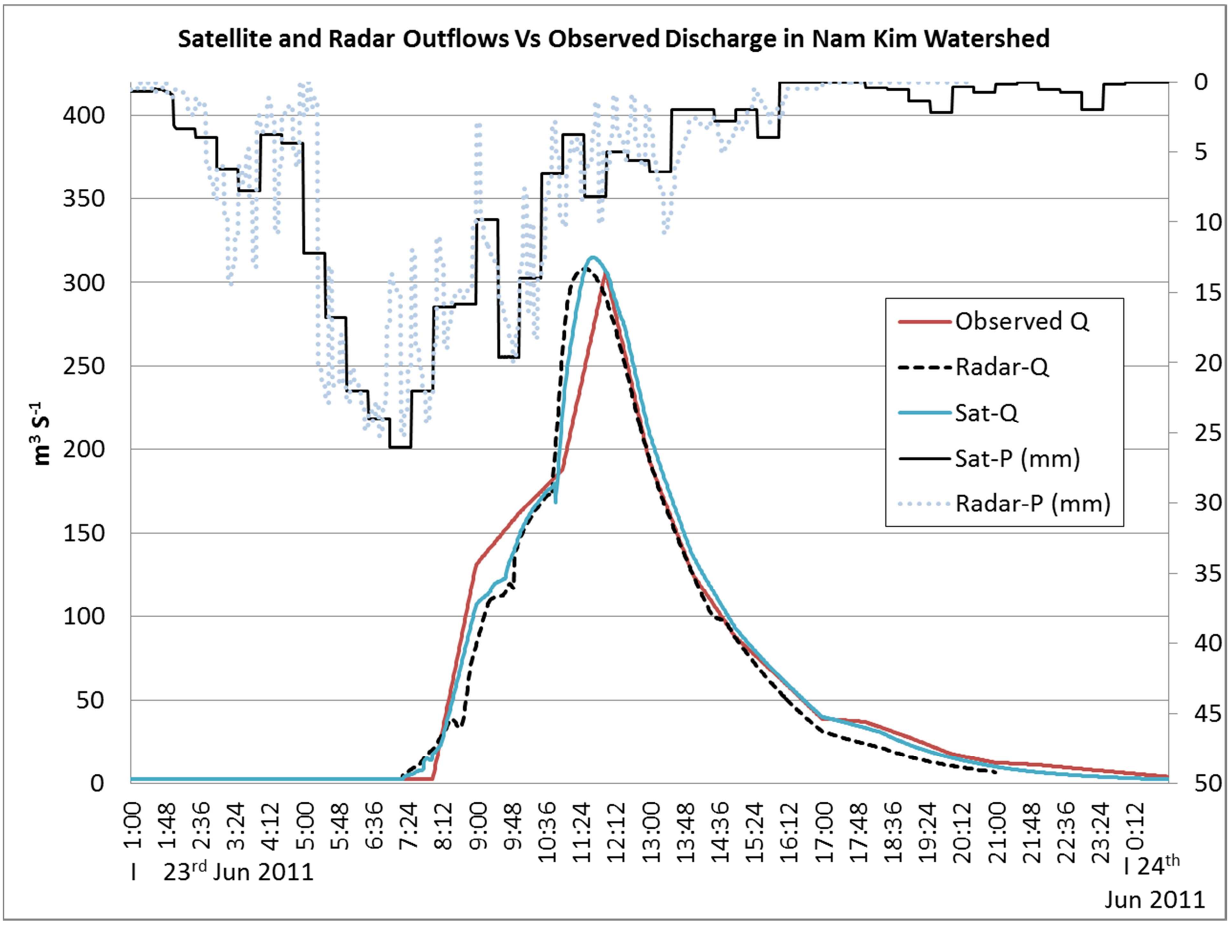

Figure 3: Simulated vs observed data through the outlet of Nam Kim watershed.

Fig. 3 showed a good agreement between the model outflows and gauged data through the Nam Kim' outlet. The model was performed with hill slope Ks ranged from 4.3 to 11.5, from 6.1 to 10.7; the S was set at 0.46, 0.42 and N ranged from 0.04 to 0.1, 0.05 to 0.12 for Nam Kim and Nam Khat, respectively. The agreement is illustrated by the calculated Nash–Sutcliffe efficiency (NSE) of 0.78 for the use of satellite rainfall and 0.71 for the use of radar rainfall data. The errors of the times and the peak values comparing between simulated data and observed information were approximately 30 minutes and 10 $m^3 s^{-1}$, respectively. This would be a result of differences between the coarse time of gauged measurement (1 hour) and the time of model estimation (1 minute).

4.2. Comparisons between different rainfall inputs effecting on sediment yield

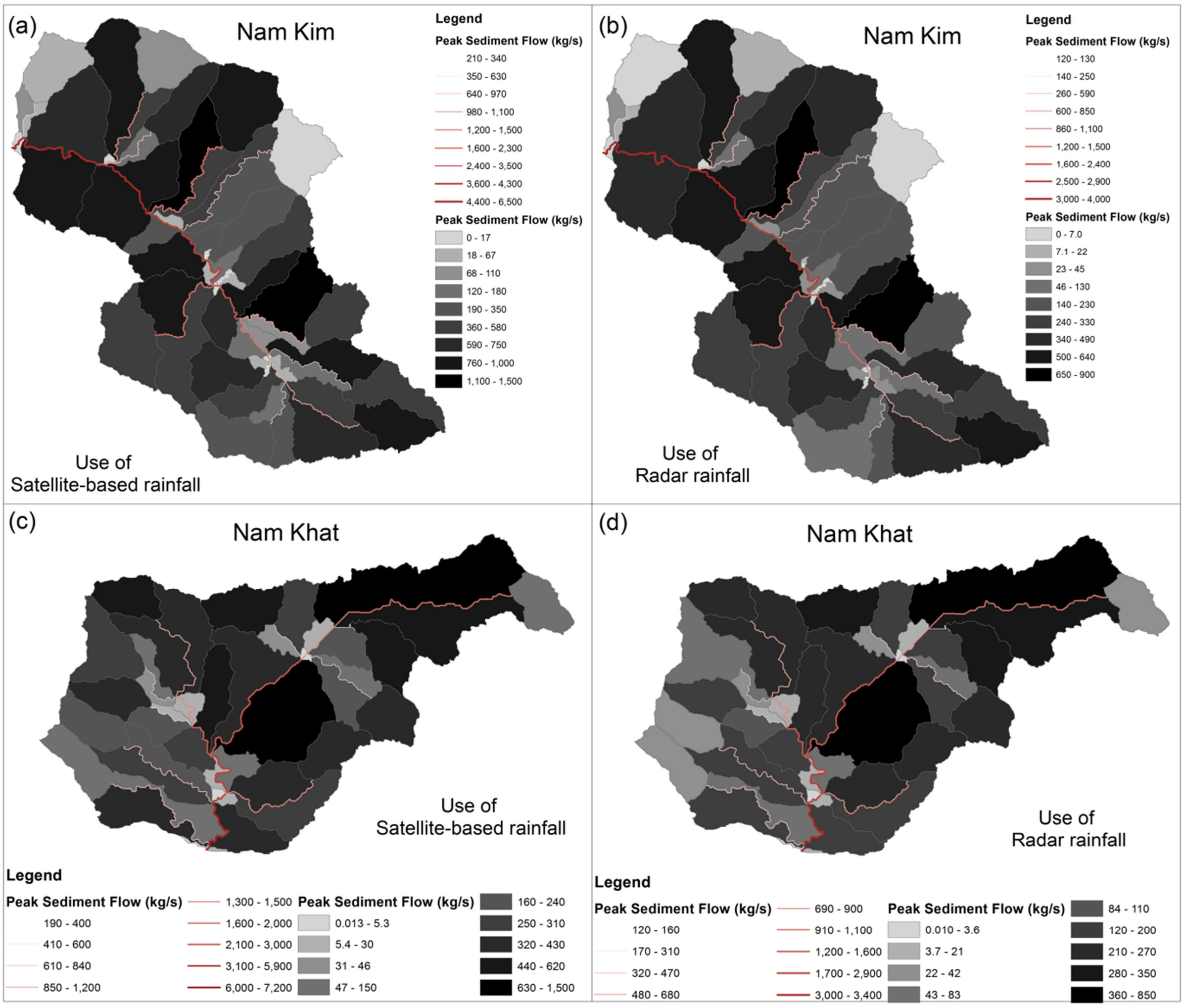

Figure 4: Rainfall inputs effect on simulated sediment flows of Nam Kim and Nam Khat watersheds for the rain event on 23rd June 2011.

The remarkable indications shown on the Fig. 4 were various patterns of the plane and channel sediment flows (SeF) and the flow volumes. Although, the pattern colors on individual watersheds (a compares to b, c to d) were not much different, the SeF values of the use of radar rainfall were much lower than the use of satellite rainfall (indicated by the legends). The rainfall is presented on the Fig. 5 and 6 with outstanding differences of temporal resolutions.

4.3. Impacts of soil saturation index on simulated soil loss for the two watersheds

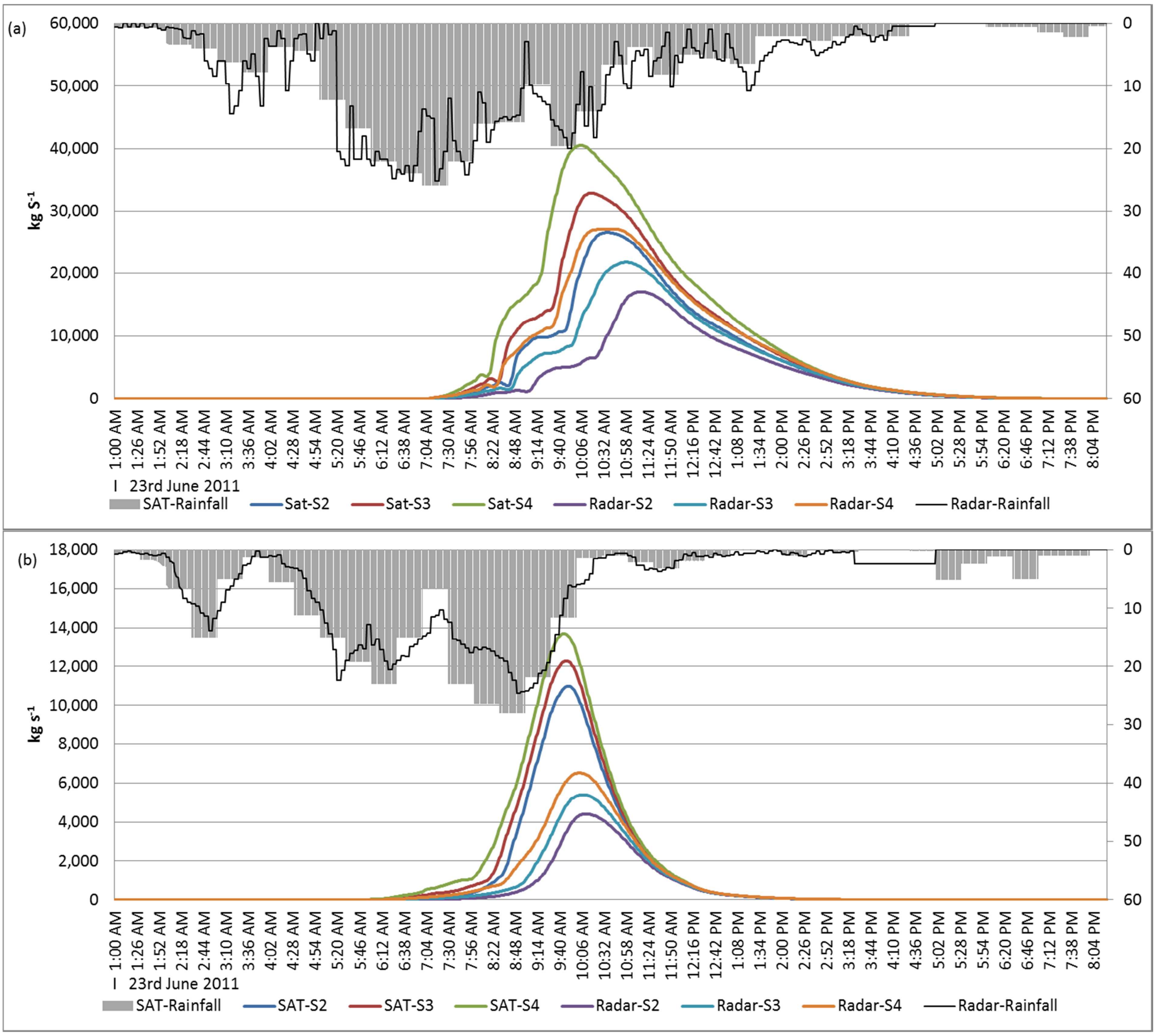

Figure 5: Peak sediment flow estimated at the outlets of Nam Kim (a) and Nam Khat (b) with variations of Soil saturation Indexes (S).

There were sharp rises (from 17 ton s^{-1} to just over 40 ton s^{-1} for the Nam Kim and from about 4 ton s^{-1} to 13.5 ton s^{-1} for the Nam Khat) of peak sediment discharges flowing through the river's outlets while the S was increased from 20% (S2) to 30% (S3) and to 40% (S4) on the Fig. 5. The Fig. 5 indicated the gradual increase of lag time to peak. However, with the bigger watershed (Nam Kim) this trend was more evident (Fig. 5a). It is also can be seen that the use of the satellite rainfall (SAT-rainfall - mm h^{-1}) produced higher sediment discharge than the use of the radar rainfall (Radar-Rainfall - mm h^{-1}).

4.4. Results of testing plane or hill slope roughness effecting on soil lost estimation

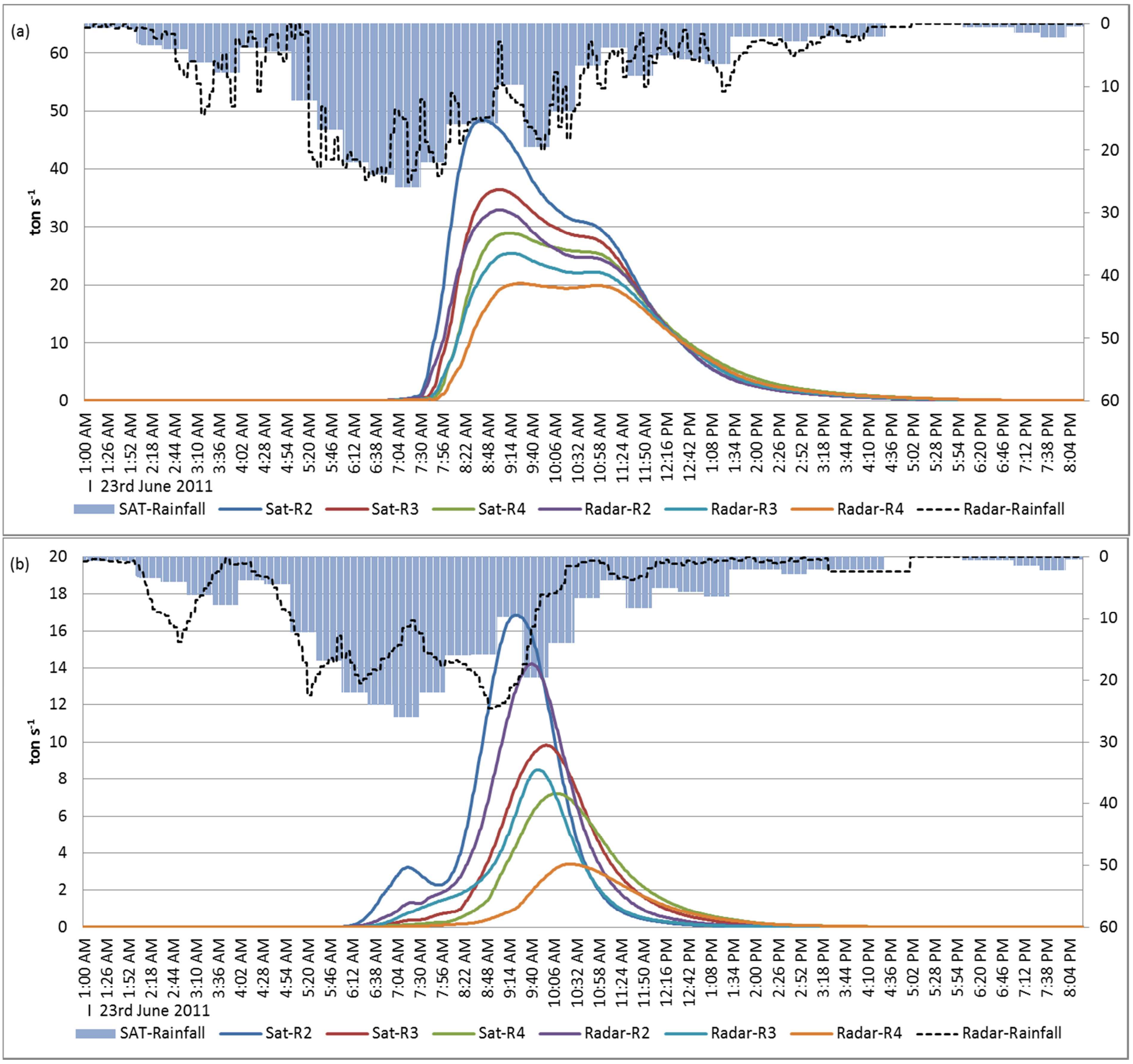

Figure 6: Peak sediment flow estimated at the outlets of Nam Kim (a) and Nam Khat (b) with variations of Plane roughness (R).

The graphs on the Fig. 6 showed the impacts of the roughness of watershed's planes on the computed sediment discharges with multipliers of 2 (R2), 3 (R3) and 4 (R4) in compassion with different climate data of precipitation. Both watersheds presented sensitive to this parameter with large scale of variations of SeF values. When comparing Fig. 5 with Fig. 6, it can be seen that the bigger catchment area of Nam Kim reserved the lateral flow while the smaller one of Nam Khat seemed to more sensitive to small rain at the very first of the whole rain event.

4.5. Effects of plane Ks on simulated soil loss

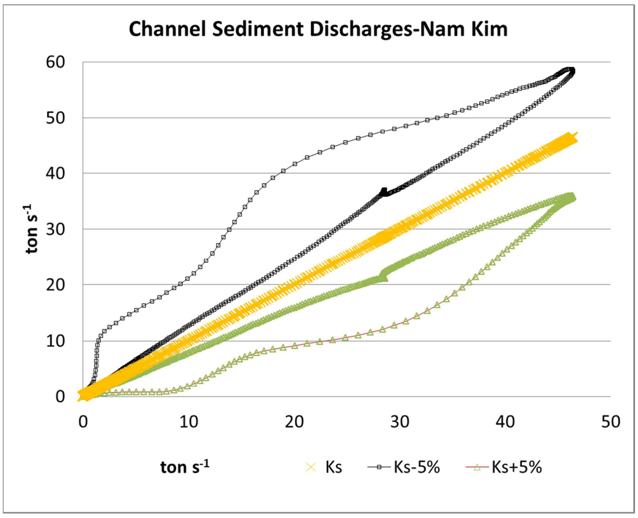

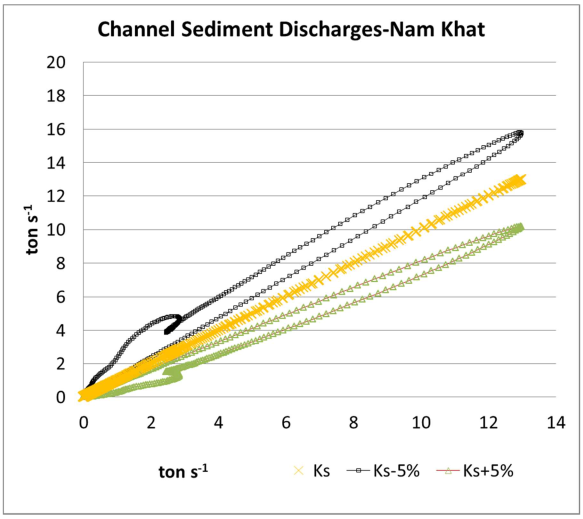

Figure 7: Evaluated total channel discharge for Nam Kim and Nam Khat watersheds with plane Ks alternations and radar rainfall input.

By adjustments the saturated hydraulic conductivity (Ks) we had comparisons between total sediment flow (TSeF) through the outlets of the two watersheds in conditions of plus and minus 5% to Ks (Ks-5% and Ks+5% to the Ks values shown within table 1 and 2). The figure 7 indicated that by minus 5% to Ks the TSeF increased significantly, particularly in the middle of the simulation time for the both cases. In the other hand, with Ks+5%, there were important sharp declines also for both watersheds. It is also shown on the graphs (Fig. 7) that, the curves were quite symmetric. This illustrated the dominant influences of Ks alternations on the TSeF volumes and minor on lag peak time.

4.6. The effect of geomorphologic resolution on modeling of channel and plane sediment yield

Interesting results of sediment yield (SeY) maps are illustrated on the Fig. 8. By the watersheds were discretized into larger components (planes) or bigger critical source areas (CSAs), the estimated sediment yield for the planes was reduced gradually in both cases. Remarkably, the channel SeFs were dropped sharply while the CSAs were enlarged. In addition, there was a significant simplification of SeY rates in small watershed components (Fig. 8a, d) into larger ones (c, f) with lower SeY rates. The figure also showed that the SeY rates were higher in upper-stream areas (about 30 ton h^{-1} for Nam Kim and around 6 ton h^{-1} for the Nam Khat) and lower in down-stream zones (approximately 3 ton h^{-1} for Nam Kim and 300 kg h^{-1} for Nam Khat) of both watersheds.

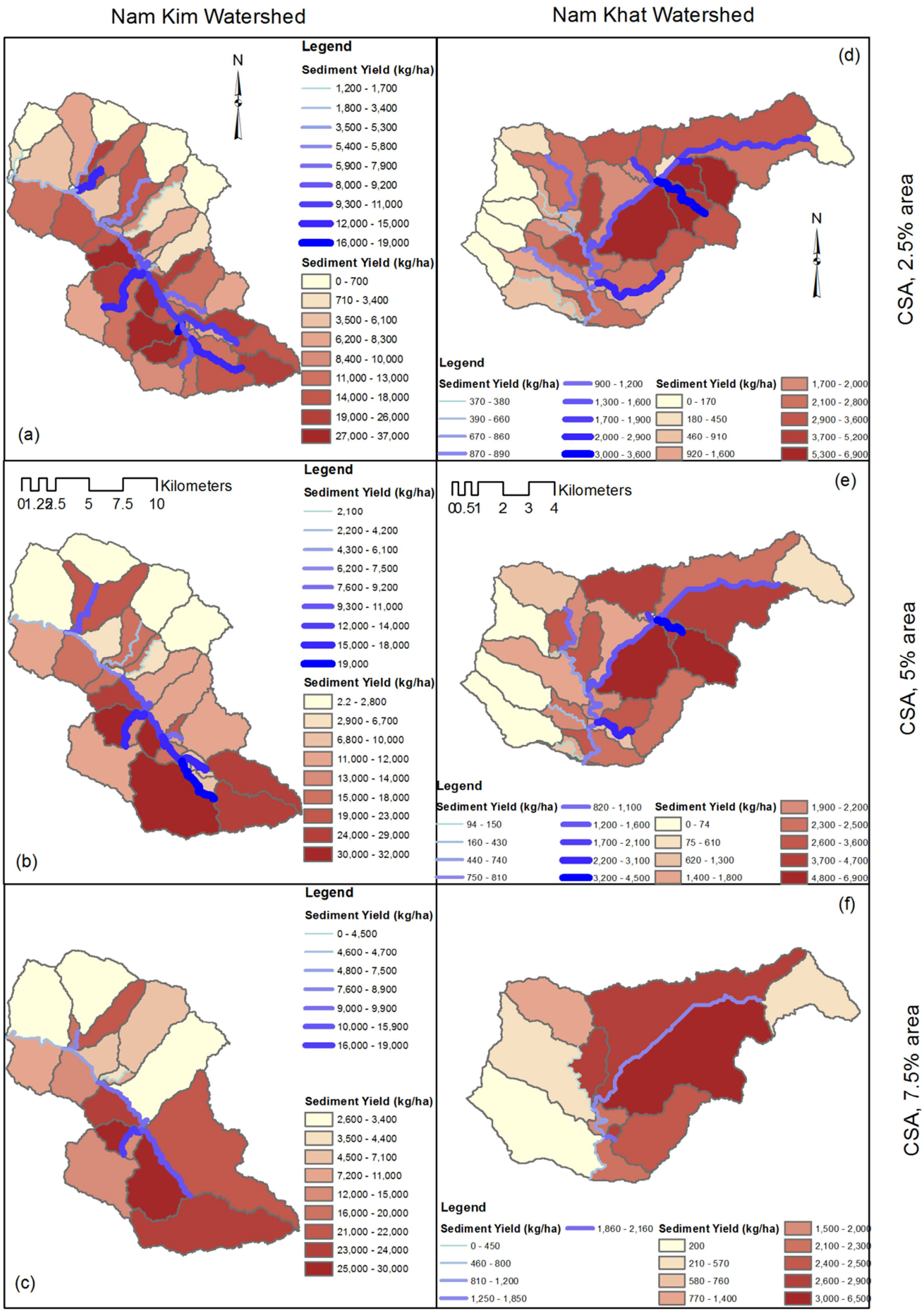

Nam Kim Watershed
Nam Khat Watershed
CSA, 2.5% area
CSA, 5% area
CSA, 7.5% area
(a)
(b)
(c)
(d)
(e)
(f)
N
Kilometers
0 1.25 2.5 5 7.5 10
0 0.5 1 2 3 4
Legend
Sediment Yield (kg/ha)
1,200 - 1,700
1,800 - 3,400
3,500 - 5,300
5,400 - 5,800
5,900 - 7,900
8,000 - 9,200
9,300 - 11,000
12,000 - 15,000
16,000 - 19,000
Sediment Yield (kg/ha)
0 - 700
710 - 3,400
3,500 - 6,100
6,200 - 8,300
8,400 - 10,000
11,000 - 13,000
14,000 - 18,000
19,000 - 26,000
27,000 - 37,000
Legend
Sediment Yield (kg/ha)
370 - 380
390 - 660
670 - 860
870 - 890
900 - 1,200
1,300 - 1,600
1,700 - 1,900
2,000 - 2,900
3,000 - 3,600
Sediment Yield (kg/ha)
0 - 170
180 - 450
460 - 910
920 - 1,600
1,700 - 2,000
2,100 - 2,800
2,900 - 3,600
3,700 - 5,200
5,300 - 6,900
Legend
Sediment Yield (kg/ha)
2,100
2,200 - 4,200
4,300 - 6,100
6,200 - 7,500
7,600 - 9,200
9,300 - 11,000
12,000 - 14,000
15,000 - 18,000
19,000
Sediment Yield (kg/ha)
2.2 - 2,800
2,900 - 6,700
6,800 - 10,000
11,000 - 12,000
13,000 - 14,000
15,000 - 18,000
19,000 - 23,000
24,000 - 29,000
30,000 - 32,000
Legend
Sediment Yield (kg/ha)
94 - 150
160 - 430
440 - 740
750 - 810
820 - 1,100
1,200 - 1,600
1,700 - 2,100
2,200 - 3,100
3,200 - 4,500
Sediment Yield (kg/ha)
0 - 74
75 - 610
620 - 1,300
1,400 - 1,800
1,900 - 2,200
2,300 - 2,500
2,600 - 3,600
3,700 - 4,700
4,800 - 6,900
Legend
Sediment Yield (kg/ha)
0 - 4,500
4,600 - 4,700
4,800 - 7,500
7,600 - 8,900
9,000 - 9,900
10,000 - 15,900
16,000 - 19,000
Sediment Yield (kg/ha)
2,600 - 3,400
3,500 - 4,400
4,500 - 7,100
7,200 - 11,000
12,000 - 15,000
16,000 - 20,000
21,000 - 22,000
23,000 - 24,000
25,000 - 30,000
Legend
Sediment Yield (kg/ha)
0 - 450
460 - 800
810 - 1,200
1,250 - 1,850
1,860 - 2,160
Sediment Yield (kg/ha)
200
210 - 570
580 - 760
770 - 1,400
1,500 - 2,000
2,100 - 2,300
2,400 - 2,500
2,600 - 2,900
3,000 - 6,500

Figure 8: Maps of channel and plane sediment yield estimated by KINEROS2 with different geomorphologic resolutions of watershed modeling.

4.6. Comparison different LULC effect on SeY

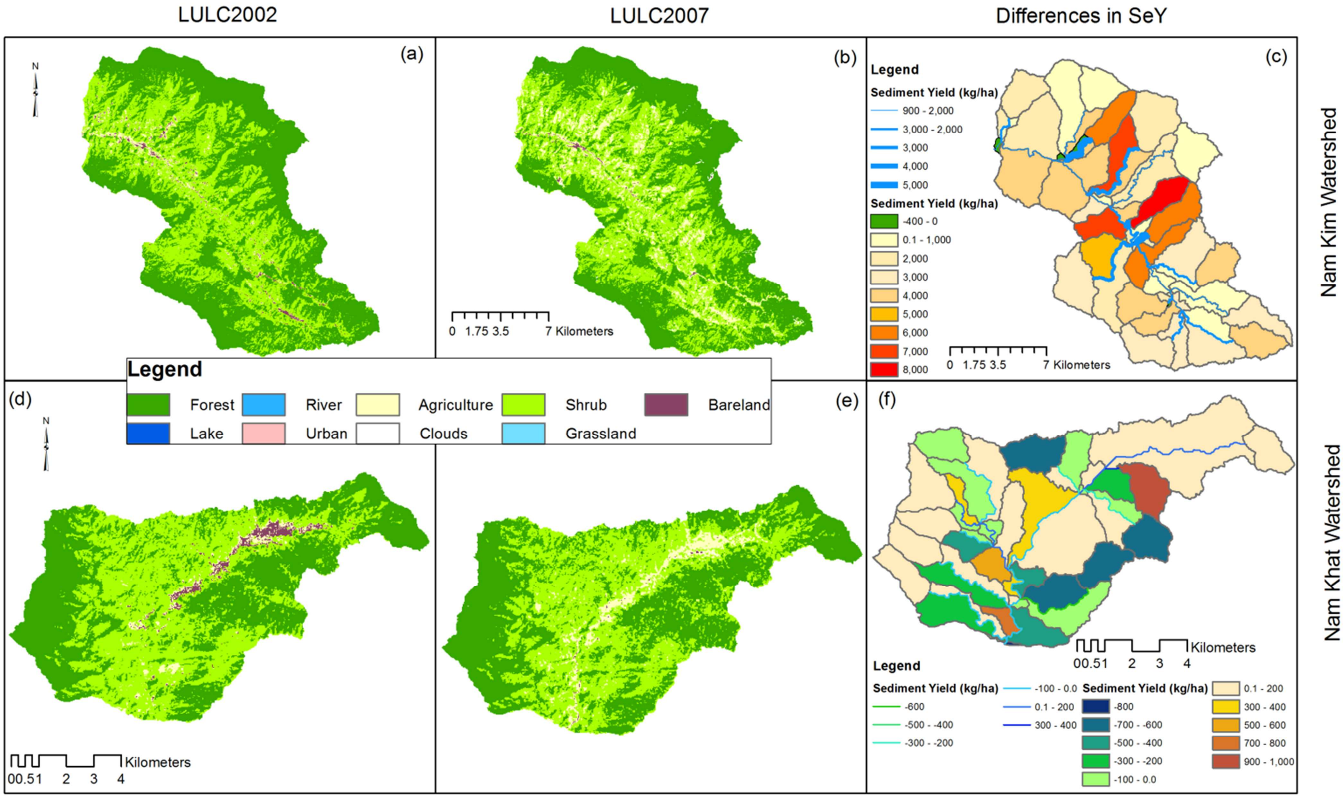

Figure 9: Maps of satellite-based LULC (a, b, d and e) and their impacts on SeY estimations (c and f) for the rain event 23rd June 2011.

The reduction of vegetation cover (decline of the forest and increase of shrub, bare and agricultural land) in five years (2002 to 2007) was clearly shown when comparing map Fig. 9a and b of Nam Kim watershed. In contrast, this was less evident on the maps of Nam Khat (d and e). Using the LULC2007 of Nam Kim generated more significant rates of sediment yield than the use of LULC2002 in most areas. In some areas (in red or orange), the soil lost rates increased from 4 ton h^{-1} to 8 ton h^{-1} and there were only small areas in down-stream zone of the Nam Kim with a decline of SeY of 0 to 400 kg h^{-1}. The sediment yield transport in channels raised in most streams. However, it is not the case for the Nam Khat with the growing and sinking SeY rates were alternated.

5. DISCUSSION

Channel discharge routine in KINEROS2 is treated by the continuity equation for one-dimensional equations presented in (Woolhiser et al., 1990) and (Smith et al., 1995). When this method applied to this study, we found that most sensitive parameters to model output of discharge were critical hydraulic conductivity (Ks), Soil saturation index (S) and less sensitive was Manning n coefficient (N). This point was supported by studies of (Al-Qurashi et al., 2008; Hadi Memarian et al., 2012). By adjustment these parameters, the KINEROS2 indicated its ability to generate channel discharge close to measured data with different types of rainfall inputs (Fig. 3).

The differences in the temporal interval of precipitations derived from satellite and radar sources have had momentous effects on results of sediment flows (Fig. 4). Despite of the variances of the accumulative rainfall depths were negligible (144 and 138 mm for satellite and radar rainfall), the calibrated SeFs using satellite rainfall were nearly double the rates of using radar rainfall. This could be explained by the exponential impact of the r factor in the equation (3) which has a direct positive influence on the splash erosion. There have been numerous investigations using radar rainfall for modeling river discharge such as (Carl L. Unkrich, 2010; Looper & Vieux, 2012; Versini, 2012; Villarini et al., 2010; Zoccatelli et al., 2010) and others. However, few attempts have analyzed the uncertainty of this parameter in term of comparison with other data sources. Although radar rainfall has some advantages of finer temporal and spatial resolutions (in comparing to satellite rainfall), it is still difficult to judge which one is more accurate than the other.

Previous literatures showed that sensitive parameter analyses might be important for hydrological modeling performances due to their common task in modeling performances and an effective way to coverage the model's results to observed data by adjusting them (Duru & Hjelmfelt, 1994). We have done parameter sensitive analyses for four model variables, namely soil saturation index (S) (section 3.3), hill slope roughness (R) (section 3.4), hill slope critical hydraulic conductivity (Ks) (section 3.4) and the CSAs (section 3.5). Every variable has had in some extend influencing on the results. However, the Ks was found the most important control parameter. The Ks and S had a significant effect on SeY magnitude (peaks), the R, on the other hand, reserved lateral flow and lengthened time to peak with the bigger watershed - Nam Kim. A similar topic of CSA assessment was carried out by (Kalin et al., 2003) and we also found a significant drop of estimated SeYs while the CSAs were increasing. What the value of the CSA is feasible? This is still a tough question. However, it is much based on areas of modeled watersheds, topographic characters, geomorphologic properties (Helmlinger et al., 1993) and hydrologic responses.

The topic of investigation into changing in LULC resulting consequences of soil erosion exaggerations has been a favorite theme for many studies, to mane few (Anh et al., 2014; Blavet et al., 2009; David et al., 2014). This study employed the LULC (2002-2007, acquired date not on 23rd June 2011) datasets just for investigation how much different land use changes resulted in soil loss and did not necessarily present the factual soil erosion rates of these watersheds. If the LULC2001 (four years later) was inputted to the model, the SeY rates would be expected higher.

As a physics-based distributed model, KINEROS2 has its own advantages and disadvantages over a lumped parameter model (Schmengler, 2010). Based on model input data requirement, scale issues discussed in (Bakimchandra, 2011), model validation and SeY generations, we recommend a use of this model for the aim of soil water assessment with individual rain events in the tropics. Nevertheless, this study was limited at examination one single rain; more rain events should be tested for the model's verifications. However, some previous researches used this model for similar investigations (Smith et al., 1999) event case study in northern Vietnam (Ziegler et al., 2007; Ziegler et al., 2004; Ziegler et al., 2006) but with different respective.

6. REFERENCES

Al-Qurashi, A., McIntyre, N., Wheater, H., & Unkrich, C. (2008). Application of the Kineros2 rainfall–runoff model to an arid catchment in Oman. *Journal of Hydrology, 355*(1–4), 91-105. doi: http://dx.doi.org/10.1016/j.jhydrol.2008.03.022

Anh, P. T. Q., Gomi, T., MacDonald, L. H., Mizugaki, S., Van Khoa, P., & Furuichi, T. (2014). Linkages among land use, macronutrient levels, and soil erosion in northern Vietnam: A plot-scale study. *Geoderma, 232–234*(0), 352-362. doi: http://dx.doi.org/10.1016/j.geoderma.2014.05.011

Arnold, J. G., J.R. Williams, R. Srinivasan, K.W. King, and R.H. Griggs. (1994). SWAT: Soil Water Assessment Tool. U. S. Department of Agriculture, Agricultural Research Service, Grassland, Soil and Water Research Laboratory. *Temple, TX*.

Bakimchandra, O. (2011). Integrated Fuzzy-GIS approach for assessing regional soil erosion risks. *PhD thesis*.

Blavet, D., De Noni, G., Le Bissonnais, Y., Leonard, M., Maillo, L., Laurent, J. Y., . . . Roose, E. (2009). Effect of land use and management on the early stages of soil water erosion in French Mediterranean vineyards. *Soil & Tillage Research, 106*(1), 124-136. doi: DOI 10.1016/j.still.2009.04.010

Burns, I. S., Scott, S. N., Levick, L. R., Semmens, D. J., Miller, S. N., Hernandez, M., . . . Kepner, W. G. (2008). Automated Geospatial Watershed Assessment (AGWA) Documentation. *U.S. Department of Agriculture, Agricultural Research Service*.

Carl L. Unkrich, M. S., Chad Kahler, David C. Peter Troch, Hoshin Gupta,Thorsten Wagener, Soni Yatheendradas. (2010). Real-time Flash Flood Forecasting Using Weather Radar and Distributed Rainfall-Runoff Model. *2nd Joint Federal Interagency Conference, Las Vegas, NV*.

Cooper, J. R., Wainwright, J., Parsons, A. J., Onda, Y., Fukuwara, T., Obana, E., . . . Hargrave, G. H. (2012). A new approach for simulating the redistribution of soil particles by water erosion: A marker-in-cell model. *Journal of Geophysical Research-Earth Surface, 117*. doi: Artn F04027 Doi 10.1029/2012jf002499

da Silva, G. R. V., de Souza, Z. M., Martins, M. V., Barbosa, R. S., & de Souza, G. S. (2012). Soil, Water and Nutrient Losses by Interrill Erosion from Green Cane Cultivation. *Revista Brasileira De Ciencia Do Solo, 36*(3), 963-970.

David, M., Follain, S., Ciampalini, R., Le Bissonnais, Y., Couturier, A., & Walter, C. (2014). Simulation of medium-term soil redistributions for different land use and landscape design scenarios within a vineyard landscape in Mediterranean France. *Geomorphology, 214*(0), 10-21. doi: http://dx.doi.org/10.1016/j.geomorph.2014.03.016

Duru, J. O., & Hjelmfelt, A. T. (1994). Investigating Prediction Capability of Hec-1 and Kineros Kinematic Wave Runoff Models. *Journal of Hydrology, 157*(1-4), 87-103. doi: Doi 10.1016/0022-1694(94)90100-7

Engelund, F., & Hansen, E. (1967). A monograph on sediment transport in alluvial streams. *Teknisk Vorlag, Copenhagen, 62 pp.*

Guzman, G., Quinton, J. N., Nearing, M. A., Mabit, L., & Gomez, J. A. (2013). Sediment tracers in water erosion studies: current approaches and challenges. *Journal of Soils and Sediments, 13*(4), 816-833. doi: DOI 10.1007/s11368-013-0659-5

Hadi Memarian, Siva K. Balasundram, Jamal B. Talib, Christopher Teh Boon Sung, Alias Mohd Sood, & Abbaspour, K. C. (2012). KINEROS2 application for land use/cover change impact analysis at the Hulu Langat Basin, Malaysia. *Water and Environment Journal. Print ISSN 1747-6585*. doi: doi:10.1111/wej.12002

Helmlinger, K. R., Kumar, P., & Foufoula-Georgiou, E. (1993). On the use of digital elevation model data for Hortonian and fractal analyses of channel networks. *Water Resources Research 29,*

2599–2613.
Horton, R. E. (1933). The role of infiltration in the hydrologic cycle. *Eos Trans. AGU 14, 446–460.*
Kalin, L., Govindaraju, R. S., & Hantush, M. M. (2003). Effect of geomorphologic resolution on modeling of runoff hydrograph and sedimentograph over small watersheds. *Journal of Hydrology, 276*(1–4), 89-111. doi: http://dx.doi.org/10.1016/S0022-1694(03)00072-6
Kefi, M., Yoshino, K., & Setiawan, Y. (2012). Assessment and mapping of soil erosion risk by water in Tunisia using time series MODIS data. *Paddy and Water Environment, 10*(1), 59-73. doi: DOI 10.1007/s10333-011-0265-3
Kefi, M., Yoshino, K., Setiawan, Y., Zayani, K., & Boufaroua, M. (2011). Assessment of the effects of vegetation on soil erosion risk by water: a case of study of the Batta watershed in Tunisia. *Environmental Earth Sciences, 64*(3), 707-719. doi: DOI 10.1007/s12665-010-0891-x
Looper, J. P., & Vieux, B. E. (2012). An assessment of distributed flash flood forecasting accuracy using radar and rain gauge input for a physics-based distributed hydrologic model. *Journal of Hydrology, 412*, 114-132. doi: DOI 10.1016/j.jhydrol.2011.05.046
M. A. Nearing, G. R. Foster, L. J. Lane, & Finkner, S. C. (1989). A Process-Based Soil Erosion Model for USDA - Water Erosion Prediction Project Technology.
Millington, A. C. (1986). Reconnaissance scale soil erosion mapping using a simple geographic information system in the humid tropics. *In: W. Siderius, ed. Land evaluation for land-use planning and conservation in sloping areas. the Netherlands: ILRI, 64□81.*
Nash, J. E., & Sutcliffe, J. V. (1970). River flow forecasting through conceptual models 1: a discussion of principles. *Journal of Hydrology 10 (3), 282–290.*
NCHMF. Vietnamese National Center for Hydrological Forecasting *http://www.nchmf.gov.vn/web/vi-VN/71/29/45/Default.aspx*.
Parsons, A. J., Wainwright, J., Powell, D. M., Kaduk, J., & Brazier, R. E. (2004). A conceptual model for determining soil erosion by water. *Earth Surface Processes and Landforms, 29*(10), 1293-1302. doi: Doi 10.1002/Esp.1096
Pham Thai NAM, D. Y., Shinjiro KANAE, Taikan OKI and Katumi MUSIAKE. (2003). Global Soil Loss Estimate Using RUSLE Model: The Use of Global Spatial Datasets on Estimating Erosive Parameters. *Geoinformatics, vol.14, no.1, pp.49-53, 2003*.
Schmengler, A. C. (2010). Modeling soil erosion and reservoir sedimentation at hill and catchment scale in semi-arid Burkina Faso. *PhD thesis*.
Smith, R. E., Goodrich, D. C., & Unkrich, C. L. (1999). Simulation of selected events on the Catsop catchment by KINEROS2: A report for the GCTE conference on catchment scale erosion models. *CATENA, 37*(3–4), 457-475. doi: http://dx.doi.org/10.1016/S0341-8162(99)00033-8
Smith, R. E., Goodrich, D. C., Woolhiser, D. A., & Unkrich, C. L. (1995). KINEROS – A kinematic runoff and erosion model; Chapter 20 in V.P. Singh (editor), Computer Models of Watershed Hydrology. *Water Resources Publications, Highlands Ranch, Colorado, 1130 pp*.
Tuan, V. V. (1993). Evaluation of the Impact of Deforestation to Inflow Regime of theHoaBinh Reservoir in Vietnam, Hydrology of Warm Humid Regions. *Proceedings of the Yokahama Symposium, July 1993. IAHS Publication 216, pp. 135–138.*
Versini, P. A. (2012). Use of radar rainfall estimates and forecasts to prevent flash flood in real time by using a road inundation warning system. *Journal of Hydrology, 416*, 157-170. doi: DOI 10.1016/j.jhydrol.2011.11.048
Villarini, G., Krajewski, W. F., Ntelekos, A. A., Georgakakos, K. P., & Smith, J. A. (2010). Towards probabilistic forecasting of flash floods The combined effects of uncertainty in radar-rainfall and flash flood guidance. *Journal of Hydrology, 394*(1-2), 275-284. doi: DOI 10.1016/j.jhydrol.2010.02.014
Williams, J. R. (1995). Chapter 25: The EPIC model. *p. 909-1000. In V.P. Singh (ed.) Computer models of watershed hydrology. Water Resources Publications.*

Woolhiser, D. A., Smith, R. E., & Goodrich, D. C. (1990). KINEROS, A Kinematic Runoff and Erosion Model. *Documentation and User Manual. ARS-77. USDA, ARS, Washington, DC.*
Ziegler, A. D., Giambelluca, T. W., Plondke, D., Leisz, S., Tran, L. T., Fox, J., . . . Tran Duc, V. (2007). Hydrological consequences of landscape fragmentation in mountainous northern Vietnam: Buffering of Hortonian overland flow. *Journal of Hydrology, 337*(1–2), 52-67. doi: http://dx.doi.org/10.1016/j.jhydrol.2007.01.031
Ziegler, A. D., Giambelluca, T. W., Tran, L. T., Vana, T. T., Nullet, M. A., Fox, J., . . . Evett, S. (2004). Hydrological consequences of landscape fragmentation in mountainous northern Vietnam: evidence of accelerated overland flow generation. *Journal of Hydrology, 287*(1–4), 124-146. doi: http://dx.doi.org/10.1016/j.jhydrol.2003.09.027
Ziegler, A. D., Tran, L. T., Giambelluca, T. W., Sidle, R. C., Sutherland, R. A., Nullet, M. A., & Vien, T. D. (2006). Effective slope lengths for buffering hillslope surface runoff in fragmented landscapes in northern Vietnam. *Forest Ecology and Management, 224*(1–2), 104-118. doi: http://dx.doi.org/10.1016/j.foreco.2005.12.011
Zoccatelli, D., Borga, M., Zanon, F., Antonescu, B., & Stancalie, G. (2010). Which rainfall spatial information for flash flood response modelling? A numerical investigation based on data from the Carpathian range, Romania. *Journal of Hydrology, 394*(1-2), 148-161. doi: DOI 10.1016/j.jhydrol.2010.07.019

BIOGRAPHICAL NOTES

- Name of the first author: Hong Quang NGUYEN
- 1995-2000, studying bachelor of Land survey at Hanoi University of Mining and Geology, Hanoi, Vietnam
- 2004-2007, studying master of geodesy at Hanoi University of Mining and Geology, Hanoi, Vietnam
- 2012-current, PhD program at Georg-August-University of Göttingen, Germany
- 2000-2010, working for Vietnamese Natural Resources and Environment Corporation, Hanoi, Vietnam as a geodesy engineer.

CONTACT

MSc. Hong Quang NGUYEN
Institution: Georg-August-University of Göttingen, Germany
Address: Geographisches Institut, Abteilung Kartographie, GIS und Fernerkundung
Goldschmidtstr. 5 37075, Göttingen, Germany
Tel.: +49.551-39 9805
Fax: +49. 551-39 8020
Email: hong-quang.nguyen@geo.uni-goettingen.de